

MULTI-FEED-PER-BEAM ANTENNA CONCEPT FOR HIGH-PERFORMANCE PASSIVE MICROWAVE RADIOMETERS

C. Cappellin⁽¹⁾, J. R. de Lasson⁽¹⁾, K. Pontoppidan⁽¹⁾, N. Skou⁽²⁾

⁽¹⁾TICRA, Landemærket 29, DK 1119 Copenhagen, Denmark, Email: cc@ticra.com, jrll@ticra.com, kp@ticra.com

⁽²⁾National Space Institute, Technical University of Denmark, DK 2800 Lyngby, Denmark, Email: ns@space.dtu.dk

Abstract – A 10 m reflector antenna for a conical-scan passive microwave radiometer in C band is proposed. The reflector is an offset paraboloid in light mesh technology excited in a multi-feed-per-beam configuration, so far never used in Earth observation missions. The instrument achieves 10 km footprint and 0.5 K radiometric accuracy at less than 10 km from the coast and sea ice boundary. The size and element spacing of the required feed array, and the benefits of the feed array in controlling the unwanted effects of the grating lobes generated by the triangular mesh, are shown. These results show the great advantages given by multi-feed-per-beam technology with digital beamforming for future spaceborne passive microwave radiometers for ocean observation.

I. INTRODUCTION

Spaceborne passive microwave radiometer measurements in C band allow to assess a large variety of ocean parameters, such as, for example, sea surface temperature, ocean vector winds and sea ice concentration. The radiometric resolution required for future instruments implies multiple simultaneous beams on the Earth along- and across-track, generated by either a push-broom or a scanning radiometer.

Current microwave radiometers in space operating in C band, like AMSR-2 [1] and WindSat [2], provide a spatial resolution, defined as the (average) diameter of the -3 dB footprint on ground, of around 50 km, whereas around 10 km is desirable. This requirement leads to an antenna aperture of around 10 m in diameter, which is considerably larger than any C-band radiometer system antenna flown hitherto. The constraint of a radiometric accuracy of 0.5 K on the measured brightness temperature sets a limit on the maximum cross-polar power that can be received by the instrument, requiring an antenna with very high polarization purity. In addition, this constraint implies extremely low antenna sidelobes, to allow measurements within the required accuracy as close as 10 km from the shore-line. It is noted that current microwave radiometers in space do not provide accurate measurements closer than approximately 100 km from the shore-line, due to cross-polar and sidelobe signal

contamination.

The just mentioned requirements are unfeasible for a traditional single-feed-per-beam radiometer antenna that rely on traditional feed horns [3]. They can, however, be met in a multi-feed-per-beam configuration, where each beam is generated by several feed array elements properly excited in amplitude and phase, and the same element takes part in the formation of multiple beams. Technology has developed over the past years making this a realistic scenario. For future ocean observation missions, where measuring close to land and sea ice with very high spatial resolution and radiometric accuracy is required, multi-feed-per-beam technology is therefore a strong candidate.

In this paper, we first summarize the results of the ESA contract 4000117841/16/NL/FF/gp, in which the multi-feed-per-beam concept was generalized and proven, reaching TRL 4 with a feed array breadboard of 67 array elements. Secondly, the multi-feed-per-beam concept is applied to a 10 m deployable conical scan radiometer antenna, realized in light mesh technology, working at 6.9 GHz. The achievable radiometric performances, the size of the required feed array, and the benefits of the feed array in controlling the unwanted effects of the grating lobes generated by the mesh reflector are shown. Finally, a first order power budget for the receiving system is given, showing that the number of receivers, including the beamforming processor, can be realized using present-day and low-power electronics.

II. MULTI-FEED-PER-BEAM ANTENNA: CONCEPT AND PROOF-OF-PRINCIPLE

Traditional conical scan radiometers, like AMSR-2, Windsat, MWI and ICI of MetOp-SG, use offset reflector antennas illuminated by a single-feed-per-beam array, where each feed horn in the focal plane generates one beam on the Earth. It was shown in [3] that with single-feed-per-beam technology the stringent requirements of future radiometric missions on footprint, sidelobes and cross-polar power cannot be met simultaneously, unless each feed horn illuminates the reflector edge with less than -30 dB taper, a larger footprint is accepted and the cross-polar component, inherent of a single offset reflector, is cancelled by a matched feed [4].

If the offset reflector is illuminated in a multi-feed-per-beam configuration, the challenging requirements on footprint, cross-polar power and sidelobes levels can be met simultaneously. In the proposed multi-feed-per-beam technology, a feed array, located in the focal plane and with elements properly excited in amplitude and phase, generates all necessary beams on ground. In general, the same array element takes part in the formation of multiple beams. This is realized in practice by a feed array with elements placed less than one wavelength from each other, each connected to its own receiver and A/D converter, and excited in amplitude and phase by a digital beamformer (FPGA), see Figure 1.

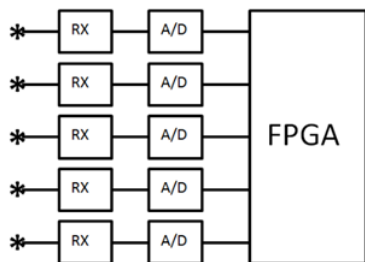


Figure 1 Multi-feed-per-beam concept. Each array element to the left is connected to its own receiver and A/D converter. The FPGA to the right combines the received signals in amplitude and phase and generates the needed beams.

In the ESA contract 4000117841/16/NL/FF/gp, completed in 2018 by TICRA with Chalmers University and DTU Space, the multi-feed-per-beam concept was proven, reaching TRL 4 with a feed array breadboard of 67 array elements. The work constituted the proof-of-concept and generalization of a previous TRP activity “Study on advanced multiple beam radiometers” (ESA contract 4000107369/12INL/MH) [5] where the electrical model of the feed array did not include mutual coupling and edge truncation effects, and the optimization algorithm, used to find the array excitations, thus considered identical element beams as input.

The feed array breadboard is constituted by 35 x-polarized and 32 y-polarized Vivaldi elements on a ground plane of 265 mm x 200 mm x 5 mm, as shown in Figure 2, and designed to operate at 6.9 GHz. The Vivaldi element was selected due to the overall cost constraints and a challenging RF modelling, and orthogonal elements were considered to have dual-linear polarization. Each Vivaldi element has a thickness of 0.4 mm and is excited by a coaxial waveguide with 50 Ω characteristic impedance. The Vivaldi element was designed by Chalmers University, who was also in charge of the breadboard manufacturing. The RF analysis of the breadboard was done in two commercial software, by TICRA in the MoM add-on to GRASP and by Chalmers University in CST, by modelling the very

detailed breadboard geometry and including mutual coupling between all elements. In Figure 3, the RF model of the breadboard developed by TICRA is displayed.

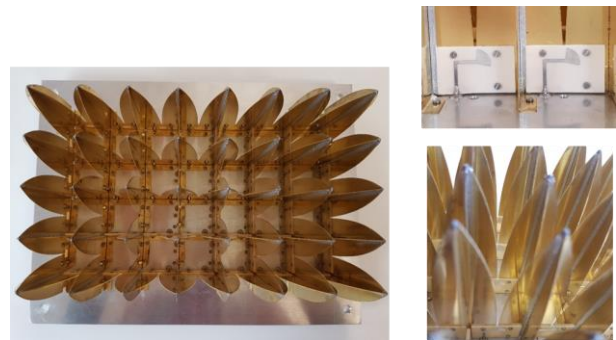


Figure 2 Feed array breadboard manufactured at Chalmers University, with details of the feeding on the right. The antenna is made of aluminum and the dielectric material for the PCB is Rogers RO4003.

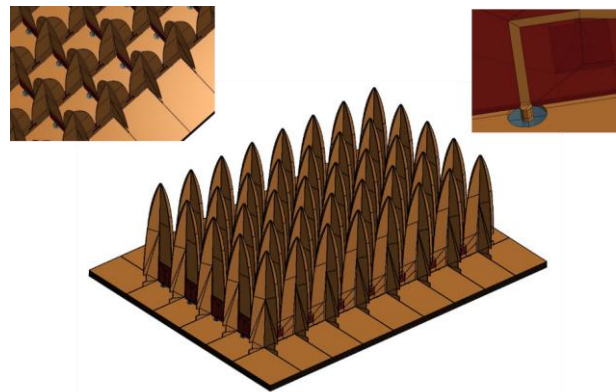


Figure 3 Model of the breadboard developed by TICRA in the MoM add-on to GRASP, with zoom on the microstrip and coaxial feeding.

Later, 14 array element patterns were measured in transmission mode in amplitude and phase at 6.9 GHz on a full sphere of 6 m radius at the DTU-ESA Spherical Near-Field Antenna Test Facility at the Technical University of Denmark [6]. One element was excited and measured at a time, with all other elements matched. A detailed comparison of the computed and measured results showed, see Figure 4 for an example and [7] for more details, that the two commercial codes provide element patterns in excellent agreement with each other and in very good agreement with the measured field in the co-polar and cross-polar components, both in amplitude and phase.

Finally, the breadboard was used to illuminate a 5 m conical-scan radiometer reflector in a multi-feed-per-beam configuration. This antenna generates two along-track beams with 30% overlap at a rotation rate of 11.5 RPM, each with a footprint of 20 km, a radiometric

accuracy of 0.25 K and a distance to coast of less than 20 km [8].

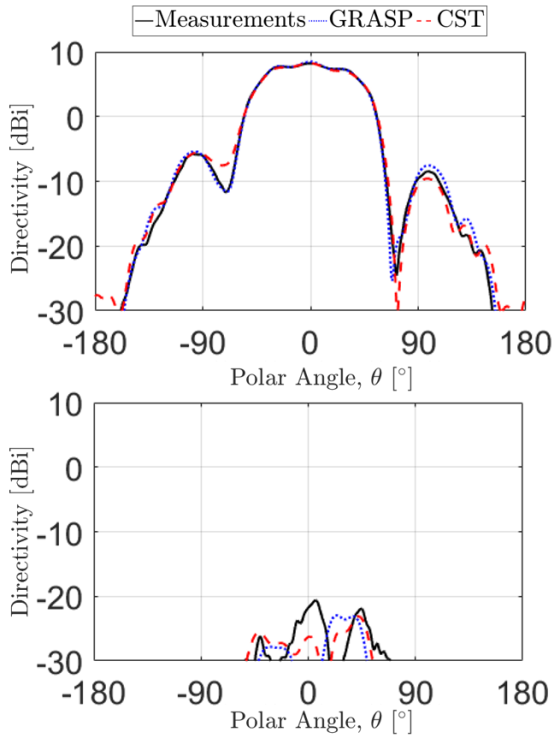


Figure 4 Directivity pattern in the $\varphi = 90^\circ$ cut for the center element of the breadboard at 6.9 GHz. Measured (GRASP) [CST] patterns shown in black (blue) [red]. The co-polar (cross-polar) component in Ludwig 3rd polarization is shown in the top (bottom) panel. The patterns refer to a coordinate system with origin at the centre of the ground plane, and with the x-axis (y-axis) parallel to the long (short) side of the breadboard.

It is noted that the multi-feed-per-beam concept requires a feed array made by closely spaced and electrically small ($< \text{one wavelength}$) elements, each connected to its own receiver and A/D converter, and properly excited in amplitude and phase by an FPGA. The Vivaldi element is used here as an example, but other elements are possible, like patches and patch-excited cups. These yield the same performance as demonstrated for the Vivaldi element here, implying that the industry is free to choose the most suitable element for future missions. One could even envision to use dual-band elements to cover several bands (C and X bands for CIMR, for example) with a single feed array [9]. As a last remark, the multi-feed-per-beam technology allows one to generate multiple beams on ground, with no or a very limited increase in the number of feed array elements. In other words, more beams do not require proportionally more feed array elements, as in the single-feed-per-beam configuration. In terms of spatial accommodation in the focal plane, the multi-feed-per-beam concept is therefore attractive, as it will

generally take up the same, or even less, space than traditional feed horns; an example comparison is presented in Section V.

III. HIGH-PERFORMANCE PASSIVE MICROWAVE RADIOMETER

A. Radiometric and antenna requirements

The initial requirements of ESA's Copernicus Imaging Microwave Radiometer (CIMR) mission are used as an example. The main objectives of the mission are to measure all weather sea ice concentration and sea surface temperature, with sub-daily coverage of the Polar regions and daily coverage of the global oceans and inland seas. This is done with a multi-frequency microwave passive radiometer, measuring in dual-linear polarization at C, X, Ku and Ka band with 0.5 K radiometric accuracy down to a distance from land and sea ice equal to the footprint. The radiometric requirements for the CIMR instrument at C band are listed in Table 1 and will be used in the following sections.

Table 1 Radiometric requirements at C band for CIMR extracted from the System Requirement Document of the 13th December 2017.

Frequency [GHz]	6.925
Footprint [km]	≤ 10
Radiometric resolution [K]	≤ 0.2
Radiometric accuracy [K]	≤ 0.5
Distance to coast [km]	≤ 10

An altitude of 817 km, an incidence angle of 53° and a swath of 1400 km are assumed. The radiometric requirements of Table 1 can be converted into antenna requirements. A footprint of 10 km implies a reflector antenna with 10 m projected aperture. A radiometric resolution of 0.2 K implies four along track beams in a conical-scan radiometer with 11.3 RPM. The radiometric accuracy is the difference between the measured and true brightness temperature. Here, we consider the signal received by the cross-polar component of the beam as the only source of error in the measured brightness temperature, when the instrument observes the sea. With this assumption it is possible to derive that a 0.5 K radiometric accuracy implies that the cross-polar power received from the Earth (or illuminating the Earth) cannot exceed 0.59% of the total power illuminating the Earth [3]. This high polarization purity requires a careful design of the feed. It is noted that additional sources of errors can play a role in the radiometric accuracy evaluation, like for example lifetime radiometric stability, which will imply an even

more stringent requirement on the cross-polar power received from the Earth. Finally, the brightness temperature of land/sea ice is higher than that of the sea, meaning that, when the instrument observes the sea in vicinity of land and sea ice, it is not enough to have high polarization purity of the beam; additionally, the sidelobes of the beam shall be as low as possible. Specifically, Table 1 states that the radiometer shall measure with 0.5 K accuracy down to 10 km from the coast/sea ice in C band. It is here assumed that this distance is measured from the -3 dB contour (footprint) of the beam, as depicted in Figure 5, and we refer to the smallest distance for which the radiometric accuracy is 0.5 K as the distance to coast. It was derived in [3] that, if the antenna beam shows negligible cross-polar power, the required accuracy of 0.5 K is obtained when the coastline is located outside the cone (with half cone angle θ_c in Figure 5) around the main beam containing 99.42% of the total co-polar power hitting the Earth. Hence, to reduce the distance to coast, one should minimize this cone.

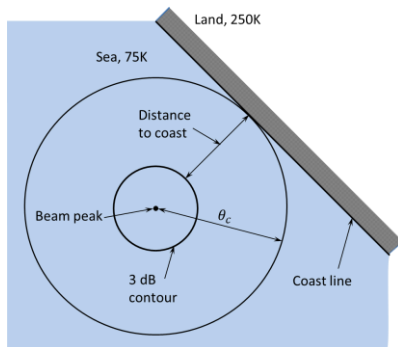


Figure 5 Footprint falling on the sea near a coast, and distance to coast definition.

B. Antenna optics and mesh reflector characteristics

In the following sections, we consider an antenna made by an offset parabolic reflector with projected aperture diameter $D = 10$ m, focal length $f/D = 0.7$, and clearance $d' = 2$ m. The reflector is first modelled as a smooth solid paraboloid, and later as a mesh reflector with a deployable ring and a cable network supporting a tensioned net covered by an RF reflective mesh (knitted mesh), as shown in Figure 6.

The surface of the mesh reflector is determined by the surface formed by the tension net, which is typically a triangulated net. The electrical properties of the mesh reflector are determined by the electrical properties of the reflective mesh, which is typically not perfectly reflective. In the following, the RF mesh will be assumed perfectly reflective. Both the shape of the triangulated net and the electrical properties of the knitted mesh have an impact on the antenna RF performance. The triangulated net consists of planar triangles with vertices lying on the nominal paraboloid.

The most commonly adopted geometry of the triangles is a uniform equilateral distribution, described by a single parameter being the side length s , which gives rise to a uniform mesh with hexagonal symmetry, as depicted in Figure 7. In the following, a uniform side length of 0.2 m and 0.5 m will be considered: these correspond to an rms surface error relative to the nominal paraboloid of 0.22 ($\lambda/100$) and 1.31 ($\lambda/100$), respectively. The correct surface predicted by mechanical tools, imposing equilibrium of the forces at the vertices of the triangulated net, is outside the scope of this work and is not considered [11].

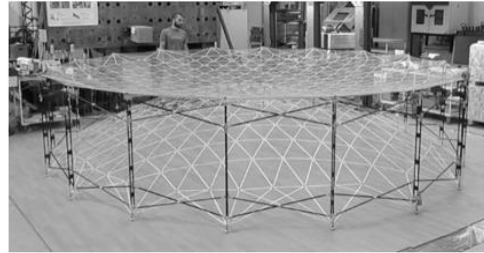


Figure 6 Double shifted pantograph ring based crossed network technology demonstrator, ESA project SCALABLE [10].

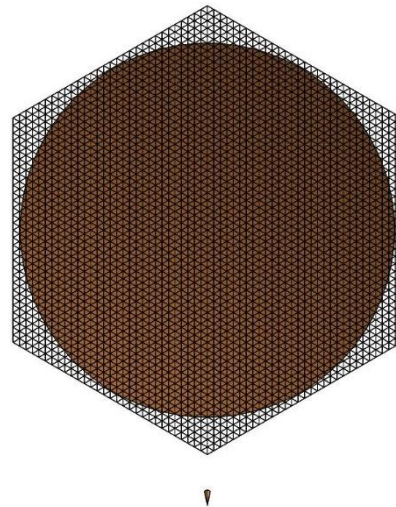


Figure 7 GRASP model of the mesh reflector surface for a parabolic reflector with $D = 10$ m, and tensioned net made with uniform planar equilateral triangles with side length $s = 0.2$ m and vertices lying on the nominal paraboloid.

IV. PERFORMANCE WITH MULTI-FEED-PER-BEAM CONCEPT

The feed array described in Section II presented a challenging RF modelling, which was computationally quite demanding. Moreover, the Vivaldi antenna is linearly polarized and has never been used in space, and thus it does not constitute a good candidate for the

CIMR feed array element, where dual-polarized antenna elements with higher TRL would be preferable. To study the benefits of a multi-feed-per-beam array for the CIMR mission, the full wave electrical model of an equivalent feed array was thus developed and used for the design. The model is constituted by 5×7 crossed half-wave dipoles located above a ground plane of 265 mm X 200 mm, displaced by 0.7 wavelength (33 mm) from each other and each excited by a coaxial feeding. It was found that the crossed dipole model performs equivalently to the Vivaldi array of Section II, for the same number of antenna elements, spacing and ground plane size, with the big advantage of being computationally much lighter than the Vivaldi array. The crossed-dipole array was placed at the focal point of the 10 m offset reflector, and the excitations of each dipole were found by the optimisation algorithm developed by TICRA in [3].

The performance of the beams generated by the multi-feed-per-beam array are shown in Table 2, for a solid reflector and a mesh reflector with uniform side lengths of 0.2 m and 0.5 m.

Table 2 Performances of the 10 m reflector antenna illuminated by 5×7 crossed dipoles in a multi-feed-per-beam scenario. Results with a nominal paraboloid and meshed surfaces with different mesh triangle side length are reported.

Multi-feed-per-beam array	Footprint [Km]	P_{cx} on Earth [%]	Distance to coast [Km]
Requirement	≤ 10	≤ 0.59	≤ 10
Nominal paraboloid	10.18	0.03	5.69
Mesh $s = 0.2$ m	10.18	0.04	5.77
Mesh $s = 0.5$ m	10.19	0.06	124.40

It is seen that the footprint is compliant and does not change when introducing the mesh reflector. Thanks to the use of dual-linear elements, the inherent cross-polar component of the offset reflector is practically cancelled, and beams with exceptional polarization purity are obtained, both with a solid and a mesh reflector. Finally, the distance to coast is less than 6 km for a smooth reflector and for a mesh reflector with $s = 0.2$ m, while it increases to more than 120 km for a mesh reflector with $s = 0.5$ m. A distance to coast of 5.77 km corresponds to a cone around the main beam with half opening angle of 0.44° . The increase in the distance to coast for a mesh reflector with $s = 0.5$ m is due to the presence of grating lobes generated by the periodic planar triangles forming the surface of the

mesh reflector. A plot of the co-polar component of one of the beams generated by the multi-feed-per-beam array with a mesh reflector with $s = 0.5$ m is shown in Figure 8. For $s = 0.5$ m the grating lobes are higher and closer to the boresight than for $s = 0.2$ m. When the grating lobes illuminate the land, they collect unwanted signal that affects the accuracy of the measured brightness temperature. To satisfy the 0.5 K radiometric accuracy, the first circle of grating lobes visible at $Az = 5.8^\circ$ and $EI = 0^\circ$, shall thus be on water. Detailed calculations show that 99.42% of the co-polar power on Earth is contained in a cone around the main beam with half opening angle of 5.9° , corresponding to a distance to coast of 124.40 km.

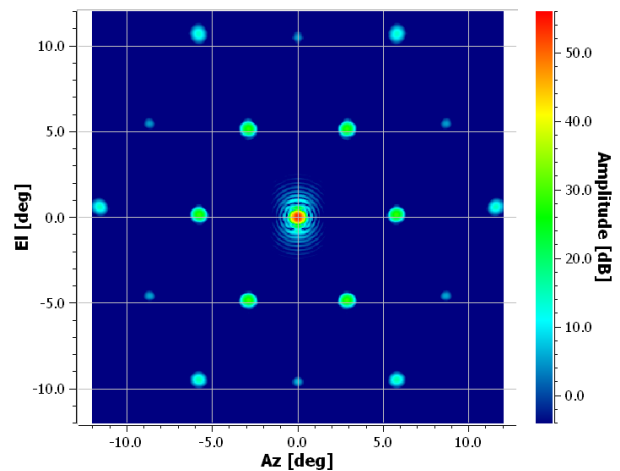


Figure 8 Co-polar component of the beam generated by the multi-feed-per-beam array with a 10 m mesh reflector, with mesh triangle side length of $s = 0.5$ m.

In general, the location of the grating lobes in the far field generated by a mesh reflector depends on the triangle side length s . For a given frequency, the larger the size s of the facets, the higher are the grating lobes and the smaller is their angular distance to the main beam. A small facet size reduces the peak of the grating lobes and moves them away from the main beam but adds mechanical complexity to the cable network. Alternatively, the use of non-regular triangular meshes can minimize the strength of the grating lobes without requiring a decrease of the (average) triangle side length [11]. It was finally found that the feed array of 35 crossed half-wave dipoles generates four compliant beams, also when the feed array is moved away from the focal point, which might be necessary to accommodate close to the focal point feeds for the higher frequencies.

The receiver system configuration and resource demands – especially concerning power consumption – is discussed and evaluated in the following, using existing state-of-the-art components. These are important issues when considering focal plane arrays: it is of little practical interest that excellent beam performance can be achieved if the receiving system

becomes impractical and too power consuming. As already noted, each antenna element is assigned its own receiver and A/D converter. Hence, the total number of components in a single receiver must be multiplied with the number of antenna elements, and further with a factor of two in order to handle two polarizations. The present system features 35 dual-polarized elements, resulting in 70 receivers.

Receivers can be designed using the direct or the super-heterodyne method. The direct layout can in principle serve C band using advanced but present day A/D converter technology. However, fast converters require much power. The super-heterodyne layout means more analog components, especially including mixer and local oscillator, but a suitable IF frequency relaxes A/D converter demands. The following component types have been addressed: Switch, low-noise amplifier, mixer, local oscillator (LO), IF amplifier, and especially A/D converter. No specific search has been made for space-qualified components, or fancy new laboratory developments – just small, low-noise commercial components. For a typical design we then find a power consumption per receiver of 860 mW, resulting in 60 W for the 70 receivers.

All receivers must use the same local oscillator signal in order to ensure coherence, and the local oscillator circuitry has an estimated power consumption of 2 W. The beam-forming takes place in FPGAs of the Virtex 5 class. The system requires 4 FPGAs each consuming about 9 W, i.e., 36 W in total.

Thus, the total power consumption for the receiver system of the 5 x 7 feed array, including beam-forming, is 98 W. This is slightly more than for a traditional receiver system handling four dual-polarized horns, but certainly not prohibitive.

V. PERFORMANCE WITH SINGLE-FEED-PER-BEAM CONCEPT

To compare the performance in Table 2 with the performance of a typical single-feed-per-beam configuration, we consider in this section a corrugated horn with a reflector-edge taper of -26 dB and aperture radius of 100 mm, and located at the focus of the 10 m reflector. The results for the generated beam, with a smooth and mesh reflector, are listed in Table 3. When comparing Table 3 with Table 2, we see that the footprint is almost identical and compliant when using a single horn or a multi-feed-per-beam array. However, the percentage of cross-polar power contained in the beam is much higher for the beam coming from the horn, stemming in part from the intrinsic cross-polar component of the feed and in part from the offset nature of the reflector configuration. The biggest difference between Table 3 and Table 2 is the value of the distance to coast, which for the horn is not only substantially larger than the requirement, but also increases to 55.42 km already with a mesh reflector with side length of $s =$

0.2 m. At the largest value of $s = 0.5$ m, the distance to coast is larger than 1000 km. The big difference in distance to coast between the horn and the array (almost a factor of five) can be explained by looking at the beam generated by the two approaches, see Figure 9. The beam generated by the multi-feed-per-beam array shows much lower cross-polar component and sidelobes than the beam generated by the horn.

Table 3 Performance of the 10 m reflector antenna illuminated by a single corrugated horn with -26 dB taper at the reflector edge. Results with a nominal paraboloid and meshed surfaces with different mesh triangle side length are reported.

Corrugated horn -26 dB taper	Footprint [Km]	P _{cx} on Earth [%]	Distance to coast [Km]
Requirement	≤ 10	≤ 0.59	≤ 10
Nominal paraboloid	10.72	0.49	25.48
Mesh s=0.2 m	10.72	0.49	55.42
Mesh s=0.5 m	10.72	0.51	1341

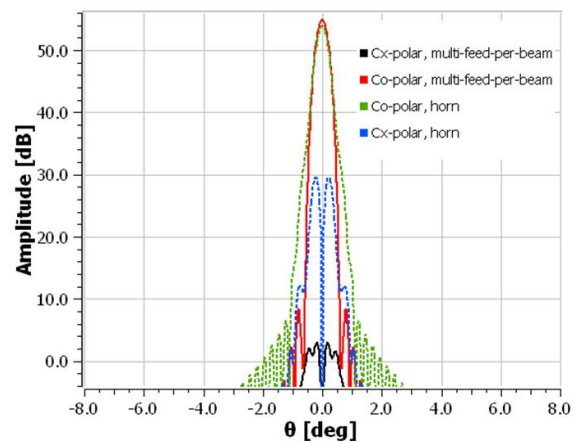


Figure 9 Co- and cross-polar components of the beam generated by the -26 dB edge taper corrugated horn (green and blue curves) and the 265 mm X 200 multi-feed-per-beam array of Section IV (black and red curves)

It is finally interesting to compare the size of the multi-feed-per-beam array described in Section IV, able to generate four compliant beams with 20% footprint overlap, to the size of the four corrugated horns generating one beam each, see Figure 10. It is seen that the 265 mm x 200 mm feed array occupies less space on the focal plane than the 400 mm x 700 mm area needed by the four corrugated horns.

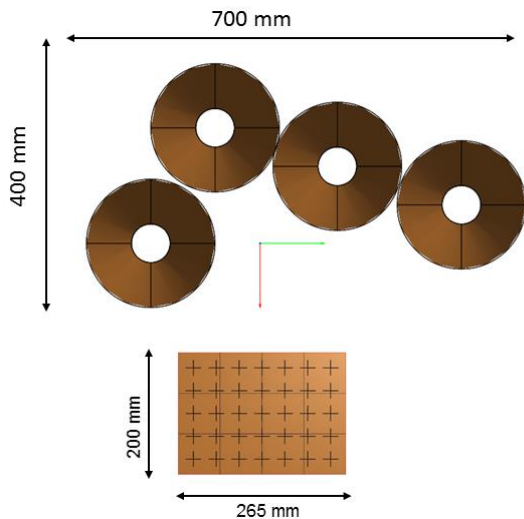


Figure 10 Spatial occupation of the four single-feed-per-beam horns in C band and the multi-feed-per-beam array analyzed in Section IV and V.

VI. CONCLUSIONS

A multi-feed-per-beam array illuminating a 10 m deployable mesh reflector antenna for a conical-scan microwave radiometer in C band has been proposed. The feed array generates four along track beams on the Earth and is constituted by 35 dual-linearly-polarized array elements, displaced 33 mm from each other and located on a ground plane of 265 mm x 200 mm. The instrument achieves 10 km footprint and 0.5 K radiometric accuracy at less than 10 km from the coast and sea ice boundary, satisfying all radiometric requirements initially set for ESA's CIMR mission. The performances of the multi-feed-per-beam array are superior in terms of achieved radiometric accuracy on the ocean and in vicinity of land and sea ice, relative to four high performance corrugated horns in a traditional one-feed-per-beam configuration. Moreover, the multi-feed-per-beam array allows the use of 20 cm average side length in the mesh reflector realization, while keeping compliant performances despite the grating lobes arising from the mesh reflector. These results show the great advantages given by multi-feed-per-beam technology with digital beamforming for future spaceborne passive microwave radiometers for ocean observation.

VII. REFERENCES

- [1] <http://www.remss.com/missions/amr/>
- [2] <http://www.remss.com/missions/windsat/>
- [3] O. Iupikov et al., "Multi-Beam Focal Plane Arrays with Digital Beamforming for High Precision Space-Borne Ocean Remote Sensing", *IEEE Trans. on Antennas and Propagat.*, Vol. 66, No. 2 February 2018.

- [4] M. F. Palvig et al., "Demonstration of TM₀₁ Circular Waveguide Mode in Matched Feeds for Single Offset Reflectors", in *Proc. APS/URSI Symposium*, Boston, USA, 2018.
- [5] C. Cappellin et al., "Novel Multi-Beam C. Cappellin et al., "Design of a push-broom multi-beam radiometer for future ocean observations", in *Proc. EuCAP Conference*, Lisbon, Portugal, 2015.
- [6] DTU-ESA Spherical Near-Field Antennas Test Facility, http://www.ems.elektro.dtu.dk/research/dtu_esa_facility
- [7] C. Cappellin et al., "Feed Array Breadboard for Future Passive Microwave Radiometer Antennas", in *Proc. EuCAP Conference*, London, UK, 2018.
- [8] J. R. de Lasson et al., "Innovative Multi-Feed-per-Beam Reflector Antenna for Space-Borne Conical Scan Radiometers", in *Proc. APS/URSI Symposium*, Boston, USA, 2018.
- [9] N. Prema et al., "Design of multiband microstrip patch antenna for C and X band", *Optik*, Vol. 127, No. 20, 2016.
- [10] C. Cappellin et al., "Large Mesh Reflectors with Improved Pattern Performances", in *ESA Antenna Workshop*, Noordwijk, The Netherlands, 2016.
- [11] J. R. de Lasson et al., "Advanced Techniques for Grating Lobe Reduction for Large Deployable Mesh Reflector Antennas", in *Proc. APS/URSI Symposium*, San Diego, USA, 2017.